JOPAT Vol 23(2), 1491-1515, July – December, 2024 Edition.
ISSN2636 – 5448 https://dx.doi.org/10.4314/jopat.v23i2.8

MOLECULAR DOCKING AND ADMET PROFILING OF CARBAZOLE-RHODANINE HYBRID AS ANTICANCER AGENT

Erazua A. Ehimen[1] *, Ayodeji A. Olaseinde [2], Abel K. Oyebamiji [3],

Oluwakemi Ebenezer [4], David Adekunle [3], Adesoji A. Olanrewaju [3],

Omowumi T. Akinola [5], Samson O. Afolabi [6]

[1] Department of Chemistry, University of Ibadan, Oyo State, Nigeria.

[2] Department of Material Science and Engineering, Clemson University, South Carolina, USA.

[3] Industrial Chemistry Programme, Bowen University, PMB 284, Iwo, Osun State, Nigeria.

[4] Department of Physics, University of Alberta, Edmonton, AB T6G 2E1, Canada

[5] Microbiology Programme, Bowen University, PMB 284, Iwo, Osun State, Nigeria.

[6] Infochemistry Scientific Center, ITMO University, Saint Petersburg, 191002, Russia

Abstract

Drug resistance and lack of specificity of currently available chemotherapeutics for cancer cells contribute to the failure of cancer chemotherapy. This highlights the pressing need to develop novel anticancer agents. This research aims to investigate the inhibiting potential of Carbazole and rhodanine derivatives against Human papillomaviruses (HPVs) and Breakpoint Cluster Region (BCR), with Abelson murine leukemia (ABL) tyrosine kinase to manage human cervical cancer and human chronic myeloid leukemia (CML), respectively. Some carbazole-rhodanine hybrids were evaluated in silico against human cervical cancer (Hela) and human CML (K562) cells. In this study, Molecular docking was used to determine binding affinity, bonding, and nonbonding interaction between the studied compounds and the target. Additionally, in-silico ADMET (adsorption, distribution, metabolism, excretion, and toxicity) screening was performed to explore the bioavailability, pharmacokinetic properties, and toxicity of the carbazole-rhodanine hybrids. The structure of the compounds was also discussed relative to their bioactivity. The molecular docking revealed that the test compounds except **D, E,** and **L** demonstrated better binding affinity, hence better inhibition efficiency towards Hela and K562 cell lines than the reference drug (etoposide). Compound **G** with a cyano substituent showed the highest binding affinity with the two receptors used, with a binding energy of -7.9 kcal mol^{-1} against hela (6HKS) and -10.0 against K562 (5HU9). This was in accordance with the experimental result. The SAR illustrated that a strong electron-withdrawing substituent attached to the para-position of the phenyl ring increased the activity. The ADMET profiling showed that compounds **E, G,** and **J** had superior drug-likeness, pharmacokinetic, and toxicity properties. Based on the results, compound G may be a good candidate to be developed further into a therapeutic agent to treat chronic myeloid leukemia and cervical cancer.

Keywords: Carbazole, rhodamine, Structure-activity relationships, Molecular docking, ADMET

Correspondence: *Email: erazuaann@gmail.com

Introduction

Cancer, a leading global cause of death, involves unchecked cell growth due to mutation from various sources like radiation or chemicals [1,2] Current treatments include surgery, chemotherapy, immunotherapy, and radiation; their use depends on the cancer type and stage. However, these treatments have limitations like lack of specificity, potential for recurrence, and serious side effects [3-5]. Also, resistance to drugs due to immune escape or faulty cell death can render treatments ineffective [6].

Cervical cancer is a prominent issue globally, particularly in lower-income nations, causing around 311,000 deaths and 570,000 new cases in 2018 alone [1,7]. The primary cause is the human papillomavirus (HPV), a sexually transmitted virus categorized into low-risk and high-risk types [8]. Though, there are no approved treatments for HPV, three preventative vaccines exist, and they are ineffective for those already infected with high-risk HPV. Treatments for cervical intraepithelial neoplasia, an HPV consequence, include chemotherapy, immune-enhancers, radiotherapy, surgery, and cytotoxic medicines. However, their cost, limited success, side effects, and safety concerns restrict their use [9]. Chronic Myeloid Leukemia (CML), a myeloproliferative tumor, makes up 15% of adult leukemia cases, with an incidence of 1-2 per 100,000 adults [10]. It's caused by the fusion of genes BCR and ABL. BCR is known as Breakpoint Cluster Region gene, located on chromosome 22, while ABL is Abelson murine leukemia viral oncogene homolog 1, a gene located on chromosome 9. BCR and ABL are often involved in a type of genetic abnormality known as the Philadelphia chromosome, which is associated with chronic myeloid leukemia (CML). BCR-ABL fusion gene produces a protein with increased tyrosine kinase activity, which promotes cancerous growth in white blood cells [10].

Until a decade ago, CML treatment was limited to nonspecific drugs, but the discovery of tyrosine kinase inhibitors (TKIs) drastically changed the situation [11,12]. TKIs interfere with BCR-ABL protein's interaction with ATP, preventing malignant cellular proliferation, and significantly improving the 10-year overall survival rate from 20 to 80–90% [11, 13,14]. However, drug resistance and toxicity are significant challenges in CML treatment [15].

Carbazole scaffolds are key components of many bioactive compounds, they are derived from various natural sources and have been used in anti-cancer drugs for over 50 years [16-18]. Numerous carbazole derivatives are known for their diverse pharmacological activities, such as antioxidant, anti-inflammatory, anti-bacterial, anti-tumour, anticancer, anti-convulsant, anti-psychotic, and anti-diabetic properties [19-21]. Recently, carbazole hybrids, which combine carbazole and other anticancer pharmacophores into one, have been recognized for their potential to simultaneously target multiple aspects of cancer, potentially reducing side effects and drug resistance [22]. On the other hand, Rhodanine is a five-membered ring with significant importance in various fields including photochemistry and medicinal chemistry [23]. Its ability to interact with target proteins through various interactions makes it crucial in clinical settings [24]. Numerous studies have explored its potential in treating diseases such as diabetes, HIV, Alzheimer's, and cancer [25-27]. Chemical modifications of rhodanine often result in compounds with a range of biological activities [28-31].

Due to the lack of specificity of existing chemotherapeutics for cancer treatment, drug resistance, side effects, and toxicity of existing drugs, there is a need to search for more potent organic compounds with fewer side effects, and toxicity that can effectively target specific pathways involved in cancer progression. Since hybrid molecule, combining two pharmacophoric groups can yield more potent and selective drugs [32-34]. It will be interesting to investigate a hybrid of carbazole and rhodanine compounds for potential drug design for cancer treatment considering their individual reported biological activities.

Computational studies will be needed to investigate the potential anticancer activities of the carbazole and rhodanine hybrid. Computational tools help to rapidly and cost-effectively identify, design, and optimize drug

candidates with high precision. They allow researchers to explore vast chemical spaces, understand complex biological interactions, and predict the behaviour of drugs in living systems, ultimately leading to more effective, safer, and targeted therapies. Molecular docking is a computational technique used in structural biology and bioinformatics to predict the interaction between a protein and a small molecule such as a ligand. The primary goal of molecular docking is to predict the preferred orientation of a ligand when it binds to a protein's active site, which can help in understanding the strength and nature of the binding. [35]. It predicts the most stable complex formation between the target and ligand based on ligand conformations, position, and orientation in the protein's binding site [36]. ADMET is another computational tool, it stands for Absorption, Distribution, Metabolism, Excretion, and Toxicity which are key pharmacokinetic and pharmacodynamic properties aiding early detection of pharmacokinetic issues and potential drug failures. ADMET profiling helps optimize promising drug candidates and facilitates the design of safe therapeutic agents [37]. Hence, before a compound reaches the clinical stage, it should be evaluated for drug-likeness, pharmacokinetic features, and toxicity.

This study presents the results of an experiment using cheminformatics, bioinformatics, and molecular docking simulations to clarify the interactions and binding affinities between Hela and K562 cells and carbazole-rhodanine hybrids. A thorough ADMET screening was also done to identify the bioactive compounds that can be conveniently developed as possible safe anticancer therapeutic agents with no side effects. The investigation provided insightful information about the structural factors controlling a compound's ability to inhibit cancer molecular targets.

MATERIALS AND METHODS

Test Compounds

Carbazole-rhodanine hybrid are the test compounds used in this investigation (Figure. 1). Thirteen carbazole-rhodanine conjugates were obtained from the research by Jiang et al. [38]. The cytotoxic effects of these compounds against human cervical cancer (Hela) and human chronic myeloid leukemia CML (K562) cells were investigated experimentally by Jiang et al. [38]. Etoposide was selected as a reference drug for molecular docking due to its well-established mechanism of action as a topoisomerase II inhibitor, known binding mode, and its clinical relevance as an approved chemotherapeutic agent. It will serve as a benchmark for validating docking protocols, comparing the binding affinities and activities of new compounds, and guiding the design of potential new topoisomerase inhibitors.

Ligand Optimization and Preparation

Chem Professional 15.0 was utilized to create the 2D structures of the ligands, which were then stored as Structure Data Files (SDF). The structural data file of the standard (etoposide) was obtained from the PubChem database (www. pubch em. ncbi. nlm. nih. gov) [39]. To minimize the SDF format of the compounds and the standard, hydrogen ions and charges were added, and the Universal Force Field (UFF) was employed, to achieve the least energy conformation of the ligands appropriate for docking. The SDF files produced were converted to PDBQT format using the OpenBabel plugin in Pyrx workspace [40]. The ligands whose conformations represent the lowest energy states are in a more relaxed state with no significant strain. They are the most stable and most biologically relevant. These ligands were selected for molecular docking because of these unique properties.

Protein preparation

The crystal structures of Human papilloma virus type 16 protein for Hela cell (Pdb ID: 6HKS) obtained by X-RAY diffraction method, with a resolution of 2.19 Å, R-Value Free 0.247, R-Value Work 0.194, R-Value Observed 0.197 [41] and the crystal structure of potent type II BCR-ABL inhibitor for Chronic Myeloid Leukemia (Pdb ID: 5HU9) with resolution 1.53 Å, R-Value Free 0.196, R-Value Work 0.186, R-Value Observed 0.186 [42] was used for this study. The PDB format of these structures was fetched in

turns by ID into obtained via X-ray diffraction UCSF Chimera [43]. First, the non-standard residues were eliminated, including ions, water, and bounded ligands. Using the structure editing tool Chimera 1.14, the proteins were structurally reduced at 100 steepest descent steps, 0.02 steepest descent steps size (Ă), 10 conjugate gradient steps, 0.02 conjugate gradient steps size (Ă), and 10 update intervals. In addition, hydrogen bonds were introduced, solvents were eliminated, and charges were allocated using the Gasteiger force field. The proteins that were prepared were imported into the PyRx program to perform a molecular docking study.

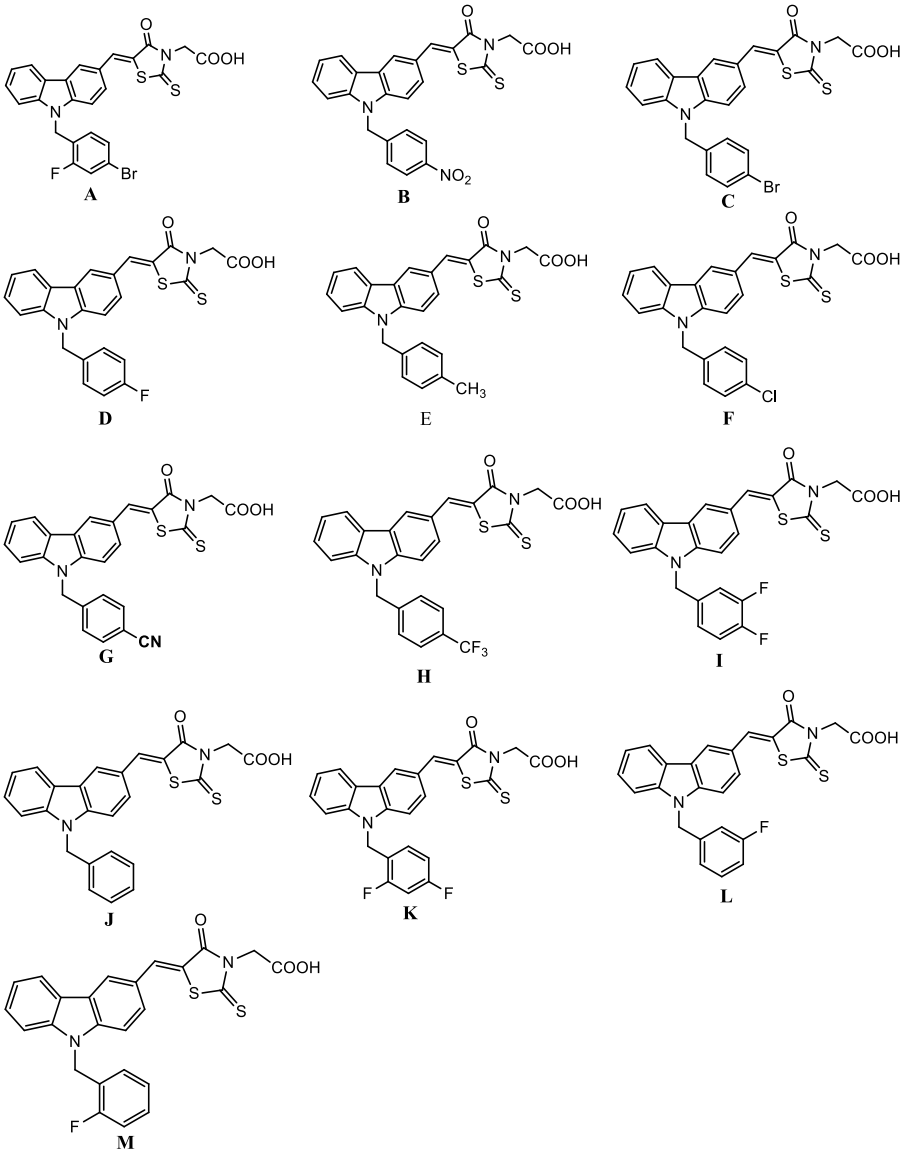

Figure1. Structure of Studied Compounds

Molecular docking

The molecular docking analysis was performed to determine the protein-ligand complex binding conformation. Using AutoDock vina in the PyRx workspace, the synthesized ligands and proteins were docked [44, 45]. Proteins that had been prepared were put into the Pyrx and converted to macromolecules. Grid space was set by focusing on significant amino acid residues in the active

site of receptors searched using Computed Atlas of Surface Topography of Proteins and UniProtKB. The grid box was set as shown in Table 1. with an exhaustiveness of 8.

Table 1: Grid box orientation

	6HKS			5HU9		
	X	Y	Z	X	Y	Z
Center	0.7999	31.1494	56.0399	-4.0093	-19.6963	-9.9817
Dimension	33.6309	39.7583	47.339	18.0876	16.1891	20.1592

Post-Docking Analysis

When the docking was complete, the binding affinity was obtained and saved as an Excel sheet. Nine conformers were considered for each ligand-enzyme complex and the conformations with the lowest binding energy (most negative value) were identified to be the best binding mode of the docked compound to the target enzyme [46]. The resulting files were uploaded for post-docking analysis to the Chimera 1.14 workspace. UCSF Chimera 1.14 was used to create 3D images of the complexes generated between proteins and ligands. The complexes generated by the docking poses of the ligands and receptors were visualized using BIOVIA Discovery Studio21, allowing for a thorough examination of the interactions and bonds that were created between them.

ADMET Screening

Absorption, distribution, metabolism, excretion, and toxicity are the pharmacokinetic features of drugs that are abbreviated to ADMET. This is referred to a pathway of how a drug is distributed in the systemic circulation and how it undergoes metabolism.

The optimal drug candidate possesses both efficacy against the therapeutic target and attractive ADMET characteristics within the therapy dose range [47]. It is intended to be swiftly absorbed from the digestive tract, transported to the body's site of action, appropriately metabolized, go through biotransformation without impairing its function, and then eliminated without causing any [37].

Lipinski's rule of five should be followed by drug-like compounds, and their lipophilicity and hydrophilicity should be balanced [48]. These regulations stipulate that: (I) there must be fewer than five hydrogen bond donors; (II) there must be fewer than ten hydrogen bond acceptors; (III) the molecular weight (MW) must be less than 500 (g/mol); and (IV) the partition coefficient Log P (CLogP) must be less than five.

In addition to the aforementioned standards, several others should be considered, such as the Veber rule [49] ((I) rotatable bond (II) PSA not greater than 140 Å), the Egan rule ((I) LOG p not more than 5.88 (II) topological polar surface area not more than 131.6 Å) [50], and the Muegge rule ((I) molecular weight 200-600 D (II) Log P between -2 to +5 (III) topological surface area not more than 150 (IV) number of rings not more than 7 (V) number of carbon atoms not less than 4 (VI) number of heteroatoms more than 1 (VII) number of rotatable bonds not more than 15) (VIII) hydrogen bond donor atoms not more than 5 and hydrogen bond acceptor atoms should be more than 10 (IX) Abbott bioavailability F should not be more than 10%) [51] when considered.

Toxicity analysis is conducted in conjunction with these investigations to comprehend any potential toxicity linked to the drug molecule that may result in specific adverse drug effects [52].

Using in silico predictive models, the test drugs' ADMET properties were ascertained. The physical and chemical characteristics, pharmacokinetics, water solubility, lipophilicity, drug-likeness, and therapeutic qualities were predicted using the SwissADME (http://www.swissadme.ch) server, a chemoinformatics-based web server [53]. The ProTox-II web-based platform was utilized to accurately forecast the toxicity of several substances [54]. PubChem (https:// pub-chem. ncbi. nlm. nih. gov) provided the canonical

SMILES for the molecular structures of all the substances.

RESULTS AND DISCUSSION

Docking Result

To determine the optimal shape and orientation of each ligand within the enzyme's active site, the docking scores calculated free binding affinities, as represented by Gibbs free energy (ΔG kcal/mol), and the interactions with each ligand's essential amino acids were investigated. Every substance that was examined demonstrated a high affinity for binding to the receptor. They engage with the amino acid residue in the receptor's active site to form an accurate match inside it. The binding energy, residues of proteins engaged in the interaction, and the distance for each complex formed are displayed in Tables 2 and 3. The 2D and 3D diagrams showing the type of interaction and the protein residues involved are also displayed in Figures 2, 3 4, and 5.

To support the research conducted through experiments by Jiang et al. [38], the test chemicals were docked to the Hela receptor's (6HKS) active site. The resulting complexes demonstrated that the test molecules inhibit the active site of the protein with binding energy between -7.0 to -7.9 Kcal/mol (Table. 2). The lower the binding affinity value of any compound, the higher the inhibiting ability of such compound [55], all the compounds' binding energies were lower than -7.3 Kcal/mol, except compounds E (-7.2 Kcal/mol) and L (7.0 Kcal/mol). This indicates that eleven compounds had better affinity to the receptor than the standard, hence they possess better anti-cancer activities. With a binding energy of -7.9 Kcal/mol, compound G exhibited the best binding interaction, this is consistent with the experimental findings of Jiang et al [38]. Van der Waal's forces of attraction and pi-alkyl bond were observed in all complexes formed. Conventional hydrogen bond was observed in all complexes formed except for compounds **E** and **L**. Pi-pi T shape was observed for compounds **A, D, K, J**, and **S.** Carbon hydrogen bonds were observed in compounds **H** and **J**. The compounds with fluorine substituent showed interaction with fluorine except for compound **F**. Pi-sigma bond was observed in complexes **C, H,** and **L**. Pi-cation was seen in complexes formed by **E, G, H,** and **J.** Only compound **B** and **F** complexes possess pi-anion and sulfur bond respectively. Since these binds involve hydrophobic and hydrogen bonds, they are essential for both the receptor-ligand interaction and for strengthening the interactions.

The test compounds were also docked to K562 (5HU9)'s active site. From the result, the compounds inhibit the active site of the Chronic Myeloid Leukemia receptor as observed from the lower value of binding affinity which ranged from -8.4 to -10 kcal/mol (Table. 3). They formed stable complexes with the receptor as shown in Figure 3. Ten of the test compounds had lower binding energy than the standard, this suggests that they can snug more perfectly into the active site of the receptor than the standard drug. Among these compounds, compound **G** had the lowest binding energy and hence possessed better anti-cancer activity. Van der Waal's forces of attraction and pi-alkyl bond were observed in all complexes formed. All the complexes that were produced, except compounds A, E, I, and M, showed conventional hydrogen bonds. Amide pi-stacked interaction was observed for compounds **C**, and I. Carbon hydrogen bonds were observed in compounds **A, B, F, G, K**, and standard drug. The compounds **D, K**, and **M** with fluorine substituent showed interaction with fluorine. Pi-sigma bond was observed in the complex formed by compounds **A, E, H, J, K, L**, and **M**. Pi-anion was seen in complexes formed by **E, C, I,** and **L**. Compound **B** and **E** complexes possess pi-cation while complexes formed by **B, E** and **K** showed interaction with sulfur. Only the standard drug and compound G showed Unfavorable donor-donor and unfavorable acceptor-acceptor, respectively. Compound A also showed pi-pi T stacked interaction. Most of the compounds in this investigation demonstrated strong binding affinities against the two cancer cell lines that were employed, suggesting that these compounds may have inhibitory effects on these macromolecules and may have potential applications as cancer treatment agents.

Table 2. Binding Affinity and Binding Interactions between Ligands and Receptor 6HKS

Ligand	ΔG kcal/mol	Hydrogen Interaction	Amino Acid Residue	Type of interactions
A	-7.7	Leu525 (4.90), Lys520 (5.27), Asn524 (4.83), Arg539 (4.30)	Val576, His572, Asn541, Gly522, Phe523, Phe521, Ile579, Lys580	Van der waals, Conventional hydrogen bond, Halogen (fourine), pi-pi T-shaped, Pi- Akyl
B	-7.8	Thr514 (3.80)	Asn541, Ser544, Asp516, Pro545, Thr548, Cys549, Ile513, Arg512, Glu589, Pro515	Van der waals, Conventional hydrogen bond, Pi-Anion, Pi-Alkyl
C	-7.4	Asp516 (4.39)	Asp524, Leu525, Ile579, Phe521, Phe523, Gly522, Asn541, Ser544, Pro545	Van der waals, Conventional hydrogen bond, pi Cation, pi-Sigma, Pi-Alkyl
D	-7.4	Gly522, Asn541 (4.55, 5.37)	Lys580, Ile579, Val576, His572, Leu525, Asn524, Phe523, Phe521, Lys520, Asp516, Pro545, Ser544	Van der waals, Conventional hydrogen bond, Halogen (fourine), pi-pi T-shaped, Pi- Akyl
E	-7.2	Nil	Asn541, Phe523, Phe521, Gly522, His572, Gly527, Gln531, Lys526, Leu526, Asn524, Ile579, Val579, Lys520, Lys580	Van der waals, pi Cation, pi-Alkyl
F	-7.7	Gly522 (5.41), Asn541	His572, Val576, Leu525, Ile579, Lys520, Phe528, Phe521, Asp516, Ser545, Asn541, Pro545, ARG539, Asn524, Lys580, Asp573	Van der waals, Conventional hydrogen bond, Sulfur-X, Pi-Sigma, Alkyl, Pi- Akyl
G	-7.9	Asn524 (5.73)	His572, Leu525, Ile579, Phe523, Phe523, Phe521, Lys520, Gly520, Gly522, Arg539	Van der waals, Conventional hydrogen bond, pi Cation, pi-pi T-shaped, Pi- Akyl
H	-7.8	Asn541 (4.03), Lys520 (4.210	Asp573, His 572, Leu525, Asn524, Phe523, Val576, Asp518, Ser544, Asp516, Gly522, Phe521, Ile579, Lys580	Van der waals, Conventional hydrogen bond, Carbon Hydrogen Bond, Halogen (fourine), Pi-Cation, Pi-Sigma, Pi- Akyl
I	-7.6	Ser538 (3.36)	Ile579, Phe521, Phe523, Lys520, Arg539, Asn524, Lys526, Leu525, Val576, Lys580,	Van der waals, Conventional hydrogen bond, Pi-Sigma, Pi- Akyl
J	-7.4	Lys520 (5.07) Asn524 (4.28)	His572, Val576, Leu525, Phe523, Arg539, Asn541, Gly522, Phe521, Lys580, Ile579	Van der waals, Conventional hydrogen bond, Carbon Hydrogen Bond, Pi-Cation, Pi-pi T-shaped, Pi- Akyl
K	-7.5	Leu525, Lys520, Asn524	Val576, His572, Arg539, Asn541, Gly522, Phe521, Phe523, Lys580, Ile579	Van der waals, Conventional hydrogen bond, Halogen (fourine), Pi-pi T-shaped, Pi- Akyl
L	-7.0	NIL	Phe523, Lys520, Gly522, Val576, Leu525, Ile579, Lys580, Asn524, Gln531, Lys526, Gly527, His572	Van der waals, Conventional hydrogen bond, Pi-Sigma, Pi- Akyl
M	-7.5	Lys520 (4.79)	Val576, Leu525, His572, Asn541, Gly522, Asn524, Phe523, Lys580, Ile579, Phe521	Van der waals, conventional hydrogen bond, halogen (fourine), pi-pi T-shaped, Pi-alkyl
Etoposide	-7.3	Asp518 (4.41), Arg539 (4.91), Phe521 (5.20), Gly522 (3.40), Phe523 (5.18)	Asn516, Asn524, Leu525, Asp573, Val576, His572, Pro545, Ser544, ASP516, Lys520	Van der waals, Conventional hydrogen bond, Akyl, Pi- Alkyl

Table 3. Binding Affinity and Binding Interactions between Ligands and Receptor 5HU9

Ligand	ΔG kcal/mol	Hydrogen Interaction	Amino Acid Residue	Type of interactions
A	-9.7	Nil	Phe359, His361, Ile360, Leu354, Val 299, Ala380, Asp381, Ile293, Leu298, Met290, Ser385, Gly383, Met278, Glu279, Leu273, Phe283, Glu282, Glu286,	Van der waals, carbon hydrogen bond, pi-sigma, pi-pi T-stacked, alkyl, pi-alkyl
B	-9.6	Asp (3.80)	Asp363, Leu387, Arg362, Lys271, Glu282, Lys285, Ile293, Va289, Glu280, Val 299, Ala380, Met290, His361, Ile360, Ser385	Van der waals, conventional hydrogen bond, carbon hydrogen bond, pi-cation, pi-sulfur, pi-alkyl
C	-9.2	Ser385 (3.33), Arg362 (3.25)	Ile360, His361, Phe359, Ile293, Lys271, Asp363, Asp381, Arg386, Gly383, Leu387, Glu282, Glu286, Lys285, Val289, Leu354	Van der waals, conventional hydrogen bond, pi anion, amide-pi stacked, alkyl, pi-alkyl
D	-8.4	His361 (4.770), Ser385 (3.19, 4.16)	Phe359, Ala380, Leu298, Val379, Met290, Asp381, Glu286, Arg386, Leu387, Asp363, Arg362, Gly383, Glu282, Ile360, Val289	Van der waals, conventional hydrogen bond, halogen (fourine), pi-anion, pi-sulfur, pi-alkyl
E	-8.6	Nil	Glu282, His361, Leu354, Ile293, Val289, Ala380, Leu298, Met290, Val379, Arg362, Asp381, Glu286, Asp363, Ser385, Leu387, Glu279	Van der waals, pi Cation, pi- anion, pi-sigma, pi-Alkyl
F	-8.9	Gly383 (5.06), Arg386 (3.76)	Lys285, Glu286, Val289, Asp381, Ser385, Leu384, glu282, Arg362, Ile360	Van der waals, conventional hydrogen bond, carbon hydrogen bond, alkyl, pi-alkyl
G	-10	Arg362 (4.37), Arg 386 (3.49)	Ile360, Phe416, Ile293, Glu282, Met388, Ser385, Gly383, Asp381, Glu286, Met290, Val289	Van der waals, conventional hydrogen bond, carbon hydrogen bond, unfavorable acceptor-acceptor, pi- akyl
H	-9.4	Arg368 (4.46), Asp381 (4.17)	Glu279, Glu282, Val289, His361, Leu354, Ile293, Val299, Ala380, Leu298, Met290, Val379, Glu286, Arg362, Asp363, Ser385, Leu387	Van der waals, conventional hydrogen bond, pi-sigma, pi- alkyl
I	-9.0	Nil	Glu282, His361, Ile360, Phe354, Leu354, Ile293, Val299, Ala380, Leu298, Met290, Val379, Arg362, Asp381, Glu286, Asp363, Ser385, Leu387, Glu279,	Van der waals, pi-anion, amide pi-stacked, pi-alkyl
J	-9.2	Asp381 (6.47)	Met290, Ile293, Val299, Val379, Ala380, Gly383, Ser385, Glu279, Glu282, Glu286, Phe 283, Ile360, Phe354, Leu354, Leu298, Val379, His361	Van der waals, conventional hydrogen bond, pi-sigma, pi- alkyl
K	-8.8	Gly383 (3.95)	His361, Leu354, Val299, Val379, Ala380, Leu298, Met290, Ile293, Asp381, Ser385, Glu286, Val379, Leu298, Phe 359, Ile360, Phe354, Leu384, Arg386	Van der waals, conventional hydrogen bond, carbon hydrogen bond, halogen (fourine), Pi-pi-sigma, pi-sulfur, pi-alkyl
L	-8.5	Gly383 (3.18)	Ile293, Leu298, His361, Leu354, Val299, Val379, Met290, Ala380, Leu298, Phe359, Ile360, Ser385, Glu282, Glu286, Asp381	Van der waals, conventional hydrogen bond, pi-anion, pi-sigma, pi-alkyl
M	-9.1	Nil	Ala380, Val379, Ile293, Leu298, Val299, Met290, Asp381, Gly383, Ser385, Arg386, Glu282, Glu286, Val289, Leu354, Phe359, Ile360, His361,	Van der waals, halogen (fourine), pi-sigma, pi-alkyl
Etoposide	-8.7	Glu286 (4.11)	Ile360, Arg362, Asp363, Ala380, Val379, Ile293, Leu298, Val299, Met290, Asp381, Val289, Lys285, Ly271, Glu286, Val289, Leu354, His361,	Van der waals, conventional hydrogen bond, carbon hydrogen bond, unfavorable donor-donor, alkyl, pi-alkyl

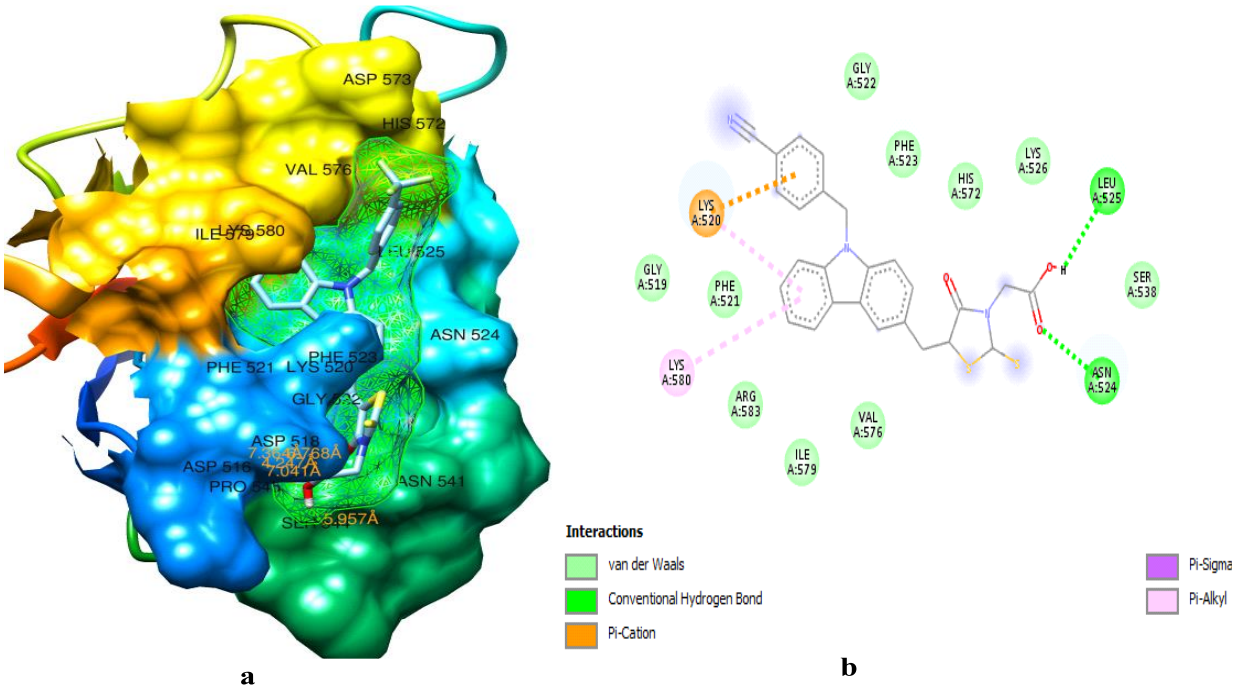

Figure 2. (a) Three-dimensional (3D) and two-dimensional (2D) views of the molecular interactions between the amino acid residues of receptor 6HKS and compound **G**

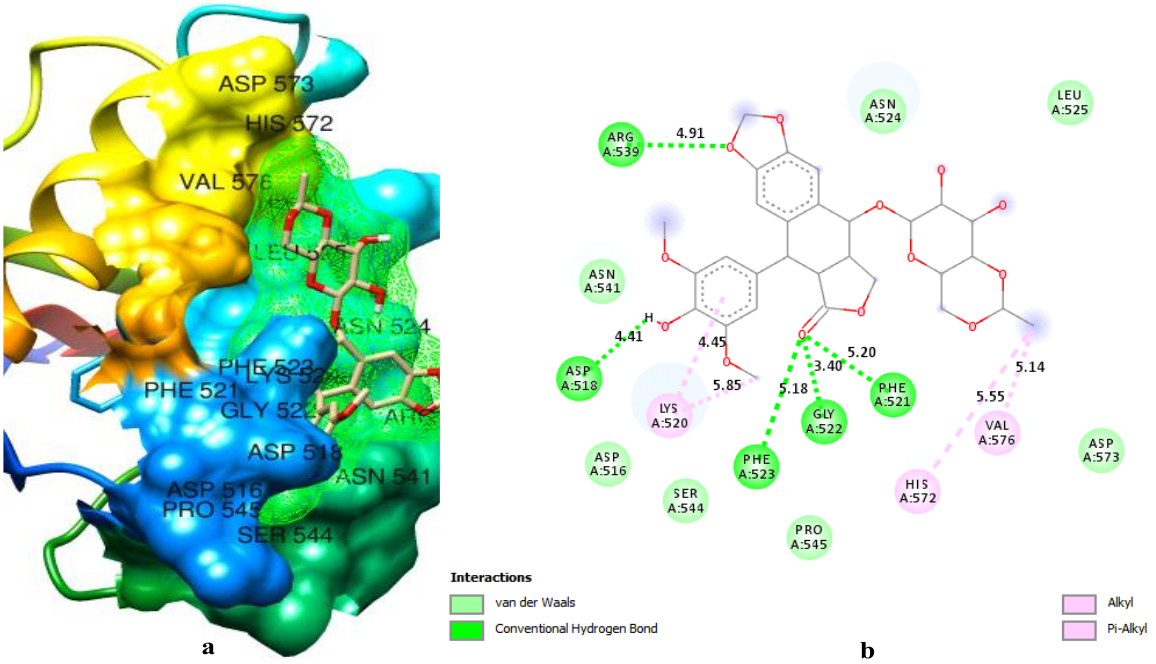

Figure 3. (a) Three-dimensional (3D) and two-dimensional (2D) views of the molecular interactions between the amino acid residues of receptor 6HKS and Etoposide

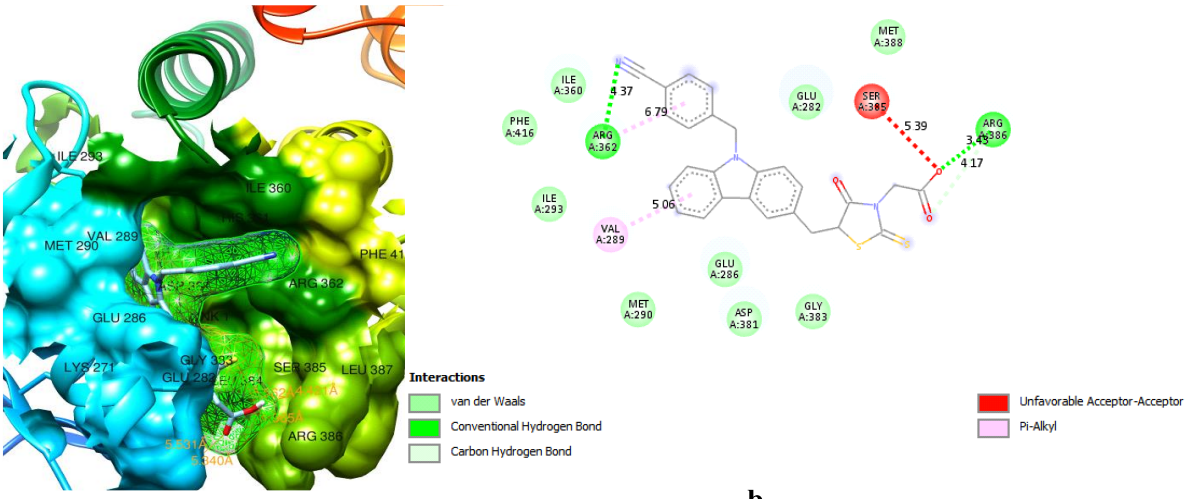

Figure 4. (a) Three-dimensional (3D) and two-dimensional (2D) views of the molecular interactions between the amino acid residues of receptor 5HU9 and compound **G**

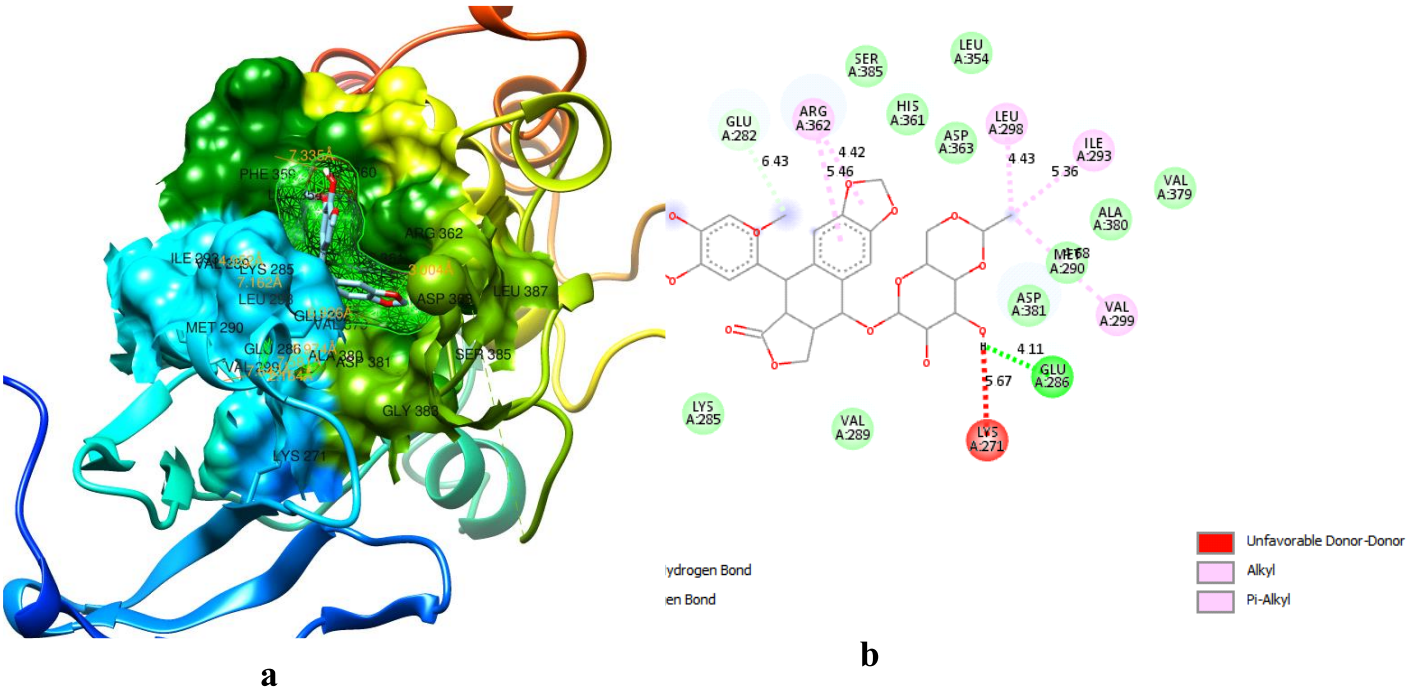

Figure 5. (a) Three-dimensional (3D) and two-dimensional (2D) views of the molecular interactions between the amino acid residues of receptor 5HU9 and etoposide

ADMET Profiling

Some of the investigated substances were observed to have the ability to inhibit the target

proteins. To assess how well they will operate pharmacologically as medications, research on their ADMET properties is required.

In silico ADMET is a rapid and affordable way to determine if a molecule will be easily absorbed, dispersed evenly to its precise site of action, positively digested, and swiftly eliminated from the body without causing any unwanted side effects is to use in silico ADMET prediction [47]. The bioactive compounds' pharmacokinetics, toxicity profiles, drug-likeness, and lipophilicity prediction outputs are shown in Tables 4, 5, 6, and 7, respectively.

Drug Likeness Analysis of the Test Compounds

Drug-likeness analysis, a qualitative measure of oral bioavailability was derived from the structural or physicochemical investigation of individual substances. Using the rule-based filters developed by Lipinski, Verber, Egan, and Muegge, the compounds' drug-likeness characteristic was assessed.

According to the rule, for a compound to have good drug-likeness and to be bioavailable upon oral administration it must not violate two or more of the rules [48,49]. The molecular weights of the test compounds range from 471.59 (E) to 588.56 (standard), with compounds A, B, C, H, and standard drugs exceeding 500 (Table 4). TPSA is the surface sum of all polar atoms, mainly oxygen and nitrogen, The test compounds had a TPSA of 57.61 Å2, with exceptions for **B** (100.75 Å2), **G** (81.4 Å2), and the standard (160.83 Å2). High TPSA and molecular weight reduce a drug candidate's penetration. However, if TPSA is < 60 Å2, absorption can exceed 90%. The molar refractivity values ranged from 135.47 (**I, K**) to 144.37 (**B).** The absorptive capacity of candidate molecules is highly dependent on the number of rotatable bonds (nRTBs). The number of rotatable bonds for test compounds and the standard is 5 except for compounds **B** and **H**. HBA ranged from 3 (**C, E, F, J**) to 13 (standard) and HBD for the test compounds is from 1 and 3 for the standard. The tested compounds have five rings and three heteroatoms (N, S, and O), some of the compounds have halogens. Etoposide has seven rings nd one heteroatom (O). The Synthetic Accessibility (SA) score, ranging from 1 (easy) to 10 (difficult), gauges a molecule's synthesis ease [56]. The examined compounds have moderate SA scores (4.37-4.49), except etoposide with a higher score of 6.27 (Table 4).

The Lipinski, Veber, Egan, and Muegge guidelines were followed by the test compounds, except the standard, which had two violations of the Lipinski and Muegge rule due to the large number of molecular weights and HBA (13) (Table 4). Therefore, the test compounds demonstrated better drug-likeness properties when compared side by side with the standard.

Table. 4: Test Compounds' Drug-Likeness Prediction Output

Code	Chemical formula	MW	RB	HBD	HBA	MR	TPSA (Å^2)	SA	Lipinski violation	Veber violation	Egan violation	Muegge violation
A	$C_{26}H_{17}BrFNO_3S_2$	554.45	5	1	4	143.21	57.61	4.38	1	0	1	1
B	$C_{26}H_{18}N_2O_5S_2$	502.56	6	1	5	144.37	100.75	4.39	1	1	1	1
C	$C_{26}H_{18}BrNO_3S_2$	536.46	5	1	3	143.25	57.61	4.39	1	0	0	1
D	$C_{26}H_{18}FNO_3S_2$	475.55	5	1	4	135.51	57.61	4.37	0	0	0	1
E	$C_{27}H_{21}NO_3S_2$	471.59	5	1	3	140.52	57.61	4.5	0	0	0	1
F	$C_{26}H_{18}ClNO_3S_2$	492.01	5	1	3	140.56	57.61	4.37	1	0	0	1
G	$C_{27}H_{18}N_2O_3S_2$	482.57	5	1	4	140.27	81.4	4.46	0	0	1	1
H	$C_{27}H_{18}F_3NO_3S_2$	525.56	6	1	6	140.55	57.61	4.49	1	0	1	1
I	$C_{26}H_{17}F_2NO_3S_2$	493.54	5	1	5	135.47	57.61	4.41	1	0	1	1
J	$C_{26}H_{19}NO_3S2$	457.56	5	1	3	135.55	57.61	4.39	0	0	0	1
K	$C_{26}H_{17}F_2NO_3S_2$	493.54	5	1	5	135.47	57.61	4.4	1	0	1	1
L	$C_{26}H_{18}FNO_3S_2$	475.55	5	1	4	135.51	57.61	4.39	0	0	0	1
M	$C_{26}H_{18}FNO_3S_2$	475.55	5	1	4	135.51	57.61	4.39	0	0	0	1
Etoposide	$C_{29}H_{32}O_{13}$	588.56	5	3	13	139.11	160.83	6.27	2	1	1	2

MW: Molecular weight; MR: Molar refractive; HBD: Hydrogen bond donor, HBA; Hydrogen bond Acceptor, TPSA: Topological Polar Surface Area; SA: Synthetic Accessibility

Lipophilicity and Water Solubility of the Studied Compounds

The partition coefficient logarithm of a drug compound in an organic or liquid phase is termed lipophilicity (Log P). It was assessed using WLOGP, XLOGP, iLOGP, MLOGP, and SILICOS-IT predictive models [57]. The arithmetic mean of the five models is referred to as the consensus log P. Lipophilicity and water solubility are critical physicochemical properties that determine the behaviors of a drug.

The lipophilicity (Log P) of a drug, is its partition coefficient in an organic phase. It is gauged using WLOGP, XLOGP, iLOGP, MLOGP, and SILICOS-IT models. Their average is known as consensus log P. Lipophilicity and solubility significantly impact a drug's behavior [58]. A drug taken orally needs to be sufficiently hydrophilic to flow through aqueous blood and enough lipophilic to cross the intestinal tract and target cell membranes. A higher Log P value signifies higher lipophilicity and lower water solubility [59]. Additionally, log P affects how well the medication molecules are absorbed by the body; a higher Log P indicates a lower level of digestion and vice versa. The tested compounds' log P values varied from 1.15 (etoposide) to 4.85 (H). The etoposide had the least log P value (1.15), this may be due to the presence of additional polar side chains in their structure. The log P value of the test compounds was observed to be higher (3.26- 4.85) due to the lack of polar side chains in their structure. As a result, all test compounds are poorly soluble while etoposide is soluble, but it is worthy of note that all test compounds and standard have log P values within the range acceptable by Lipinski, Egan, and Muegge rules.

Using the SILICOS-IT prediction model, water solubility was calculated as the logarithm of the molar solubility in water (log S). A compound's Log S value determines how well it dissolves; the higher the value, the better [60]. The compounds' Log S values varied from -3.59 (etoposide), which was soluble, to -7.59 (A), which was poorly soluble. This pattern is exactly consistent with the previously discussed Log P values.

The bioavailability score provides a semi-quantitative estimate of the likelihood that the compounds would make effective oral drug based on the total charge, TPSA, and Lipinski filter drugs [61]. With the exception of (B) 0.11 and 0.17 for etoposide, the test drugs' bioavailability scores (Table 5) from the ADME results were 0.56. Given that these compounds have a 0.55 bioavailability score, which indicates that they have a 55% chance of at least 10% oral absorption in rat or human colon cancer (Caco-2) permeability [62], these compounds are probably going to work well as oral drugs.

Table 5: Predicted Lipophilicity (Log P) Values, Water Solubility and Bioavailability of the Studied Compounds

Code	iLOGP	XLOGP3	WLOGP	MLOGP	Silicos-IT Log P	Consensus Log P	ESOL Log S	Solubility Class	BS
A	2.63	5.74	5.16	3.65	6.52	4.74	-7.59	Poorly soluble	0.56
B	2.91	3.78	4.27	1.69	3.66	3.26	-6.58	Poorly soluble	0.11
C	3.53	5.64	4.6	3.28	5.09	4.43	-7.42	Poorly soluble	0.56
D	3.21	4.05	4.4	3.08	5.84	4.11	-6.67	Poorly soluble	0.56
E	3.23	4.31	4.15	2.91	5.95	4.11	-6.81	Poorly soluble	0.56
F	3.35	4.57	5.49	3.18	6.06	4.33	-7.1	Poorly soluble	0.56
G	2.98	4.67	3.71	2.02	4.46	3.57	-6.47	Poorly soluble	0.56
H	3.45	5.83	5.01	3.48	5.5	4.85	-7.38	Poorly soluble	0.56
I	3.33	5.15	4.96	3.45	5.26	4.43	-6.84	Poorly soluble	0.56
J	3.09	4.95	3.84	2.71	4.42	3.80	-6.51	Poorly soluble	0.56
K	3.39	5.15	4.96	3.45	5.26	4.44	-6.84	Poorly soluble	0.56
L	2.38	5.05	4.4	3.08	5.84	4.15	-6.67	Poorly soluble	0.56
M	2.33	5.05	4.4	3.08	5.84	4.14	-6.67	Poorly soluble	0.56
Etoposide	3.31	0.6	1.01	-0.14	0.95	1.15	-3.75	Soluble	0.17

Pharmacokinetics Prediction of the Bioactive Compounds

All the test substances, except for J and standard, had probabilities of being absorbed in the gastrointestinal tract (GIT), according to the results of the pharmacokinetics prediction (Table 6). This implies that these substances may be absorbed in the gastrointestinal tract when taken orally [63].

The blood-brain barrier (BBB) is the primary component of medications that primarily target brain cells [64]. Both the reference and the test chemical lacked BBB permeability.

P-gp, a well-characterized ATP-binding cassette transporter in the plasma membrane, is in charge of actively egressing xenobiotics across biological membranes to shield the organism from foreign substances [65]. This efflux pump keeps some drugs from getting into sensitive areas, which leads to drug resistance. Table 6 shows that none of the test compounds or the standard are P-glycoprotein substrates, indicating that they have the potential to be effective chemotherapeutic drugs.

A superfamily of isoenzymes called cytochrome P450 monooxygenase catalyses the metabolism of many different substrates, including chemotherapy drugs. Consequently, one method for treating and preventing cancer is to use enzyme-inhibiting techniques [66]. Five main isoforms (CYP1A2, CYP2C19, CYP2C9, CYP2D6, and CYP3A4)42 have been estimated to be substrates of 50–90% of medications. The inhibition of these isoforms is a crucial factor in pharmacokinetics-related drug-drug interactions (). Due to their inability to be digested, this may lead to low bioavailability and serious side effects from their retention. The compounds have a high likelihood of undergoing transformation and being bioavailable when taken orally, as evidenced by their non-inhibition activity against these enzymes [67]. Except for etoposide, all test chemicals have the potential to inhibit CYP2C9 and CYP2D6, but none of them can inhibit CYP2D6, CYP19, or CYP1A2, indicating that they are all likely to be converted and bioavailable following oral administration.

the skin functions as a selective barrier that permits various substances to pass through at varying rates depending on their physicochemical characteristics [68]. Therefore, a crucial metric for assessing compounds that may need transdermal delivery is skin permeability (Log Kp) [69]. The molecule is less skin permeant the higher the negative log Kp value [70]). Table 6 displayed the log Kp (cm/s) of the test chemicals, with etoposide being the least permeant at -9.46 and F being the most permeant at -4.64. The results suggest that there is little skin permeability in the test substances.

Table 6: Test Compound Pharmacokinetics Prediction Output

Code	GI	BBB	P.gp	CYP 1A2	CYP2 C19	CYP2 C9	CYP2 D6	CYP3 A4	Log KP (cm/s)
A	Low	No	No	No	No	Yes	No	Yes	-4.9
B	Low	No	No	No	No	Yes	No	Yes	-5.26
C	Low	No	No	No	No	Yes	No	Yes	-4.86
D	Low	No	No	No	No	Yes	No	Yes	-4.91
E	Low	No	No	No	No	Yes	No	Yes	-4.70
F	Low	No	No	No	No	Yes	No	Yes	-4.64
G	Low	No	No	No	No	Yes	No	Yes	-5.22
H	Low	No	No	No	No	Yes	No	Yes	-4.66
I	Low	No	No	No	No	Yes	No	Yes	-4.94
J	High	No	No	No	No	Yes	No	Yes	-4.87
K	Low	No	No	No	No	Yes	No	Yes	-4.94
L	Low	No	No	No	No	Yes	No	Yes	-4.91
M	Low	No	No	No	No	Yes	No	Yes	-4.91
Etoposide	Low	No	Yes	No	No	No	Yes	No	-9.46

GI: gastrointestinal; BBB: blood rain barrier and P-gp: P-glycoprotein.

Toxicity Profiles of the Bioactive Compounds

A bioactive compound with excellent drug-likeness, lipophilicity, and pharmacokinetic properties still needs to undergo a thorough toxicity test to ensure safety and prevent side effects when administered as a drug.

Table 7 shows the chemicals' predicted levels of toxicity. Based on the ProTox II toxicity prediction, etoposide is classified as oral toxicity class 3, with an LD50 of 215 mg/kg, while all other test chemicals are classified as oral toxicity class 4, with an LD50 of 350 mg/kg.

The principal location of metabolism in humans is the liver, which may be vulnerable to the effects of numerous medications and harmful substances. Human hepatotoxicity (H-HT) illustrates many forms of liver damage that may result in the organ failing or even death [71]. All test compounds except **B, E, G, J,** and etoposide showed a tendency for hepatotoxicity. Compounds that have the potential to cause changes or malignant development through mutagenicity are identified using mutagenicity tests. Carcinogenicity substances can cause cancer by altering cellular metabolic pathways and causing harm to the DNA [72]. Among the test compounds, only compound **B** has the probability of carcinogenicity (0.54) and mutagenicity (0.78) and this may be due to the presence of nitro substituent on this compound. None of the test compounds was

cytotoxic. The detrimental effect of toxic substances on the operation of the systemic and local immune systems is known as immunotoxicity. Compounds **A, K,** and etoposide showed a tendency for immunotoxicity.

The study showed that most of the test compounds and standard compounds exhibited one type of toxicity. Compounds E, G, and J did not exhibit any tendency for hepatotoxicity, carcinogenicity, immunotoxicity, mutagenicity, or cytotoxicity, suggesting that they are safe as potential therapeutic agents.

Structure-Activity Relationship (SAR)

This structure-activity relationship (SAR) is evident in compounds **B**, **G,** and **H**, which showed good inhibiting activities against the cancer cell lines in the presence of nitro, cyano, and trifluoromethyl group substitutions group at the *para*-position of phenyl ring, respectively (Figure 6). Compounds B, G and H with stronger electron-withdrawing groups substituted on the benzyl ring displayed more potent cytotoxic activity against the studied cancer cell lines compared with compounds **C** (bromine atom) and **D** (fluorine atom) with weaker electron-withdrawing functional group substitution.

This structure-activity relationship (SAR) is evident in this study. Compounds B, G, and H demonstrate a strong inhibitory effect on the cancer cell lines when nitro, cyano, or trifluoromethyl groups are substituted at the para-position of the phenyl ring, respectively. In comparison to compounds C (bromine atom) and D (fluorine atom), which have weaker electron-withdrawing functional group substitution, compounds B, G, and H, which have stronger electron-withdrawing groups replaced on the benzyl ring, showed more significant cytotoxic activity against the examined cancer cell lines. Compound E, which has an electron-donating methyl group substitution on the benzyl ring, showed poor cytotoxic action. Compounds substituted with nitro and halogen were found to have a propensity for at least one kind of toxicity. The only compounds that did not exhibit any trend toward toxicity were compounds E, G, and J, which include methyl, cyano, and hydrogen substituents, respectively.

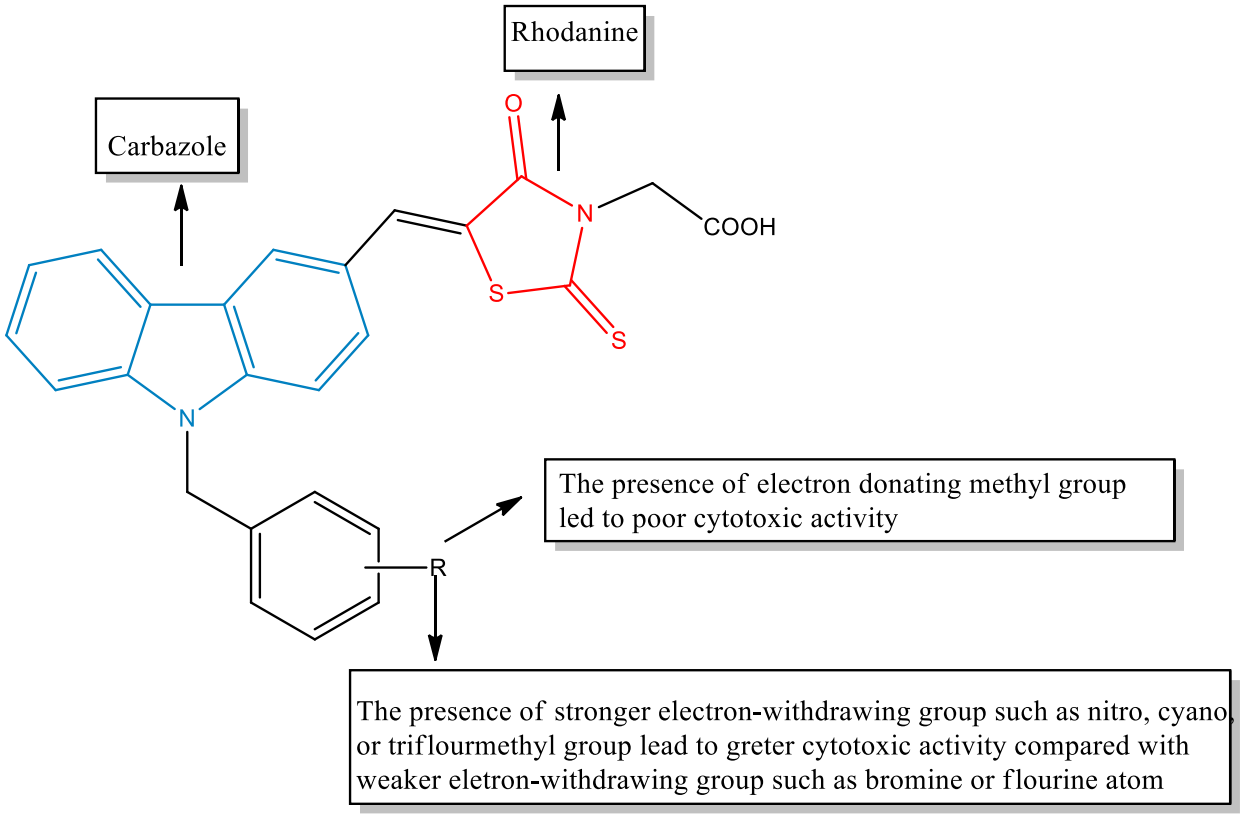

Figure 6. Structure Activity Relationship of the Test Compounds

Table 7. Toxicity Profiles of Test Compounds

Code	LD50 (mg/kg)	Toxicity Class	Hepato-toxicity	Carcinoge-nicity	Immune-toxicity	Mutage-nicity	Cytoto-xicity
A	350	4	+ (0.58)	-	+(0.91)	-	-
B	350	4	-	+ (0.54)	-	+ (0.78)	-
C	350	4	+ (0.57)	-	-	-	-
D	350	4	+ (0.57)	-	-	-	-
E	350	4	-	-	-	-	-
F	350	4	+ (0.57)	-	-	-	-
G	350	4	-	-	-	-	-
H	350	4	+ (0.54)	-	-	-	-
I	350	4	+ (0.57)	-	-	-	-
J	350	4	-	-	-	-	-
K	350	4	+ (0.57)	-	+ (0.98)	-	-
L	350	4	+ (0.57)	-	-	-	-
M	350	4	+ (0.57)	-	-	-	-
Etoposide	215	3	-	-	+(0.99)	-	-

CONCLUSION

Thirteen selected carbazole-rhodanine conjugates were investigated in silico against Hela and K562 cancer cell lines. The molecular docking studies showed that ten of the test compounds demonstrated better binding affinity, and better inhibition efficiency towards Hela and K562 cell lines compared to the standard. The SAR demonstrated an increased activity, by a strong electron-withdrawing group at the para-position of the phenyl ring. Thus, Compound **G** with a cyano substituent demonstrated the best binding affinity with the two receptors studied. The study revealed that test compounds demonstrated better drug-likeness properties compared to the standard. The pharmacokinetics showed that both the standard and the test compounds are reasonably likely to be bioavailable following oral delivery, and the lipophilicity profile showed that the standard was more soluble than the test compounds. The toxicity prediction revealed that only chemicals E, G, and J have no potential to be cytotoxic, immunotoxic, mutagenic, hepatotoxic, or carcinogenic as therapeutic agents. Among these three safe compounds, compound **G** had the best inhibitory efficiency against the two targets evaluated (6HKS and 5HU9). Hence, compound **G** is the best fit to be further developed as a safe therapeutic agent against Hela and K562 cancer cell lines. In vivo studies should be carried out to validate the toxicity profile of the compounds.

Conflicts Of Interest

There is no conflict of interest declared.

REFERENCES

[1] WHO. Cervical cancer 2021; Available at: https://www.who.int/health-topics/cervical-cancer#tab=tab_1.

[2[Pich, O., Ortes-Bullich, A., Muinos, F., Pratcorona, M., Gonzalez-Perez, A. & LopezBigas, N. (2021). The evolution of hematopoietic cells under cancer therapy, Nat. Commun. 12, 1-11.

[3] Sherin, D. R. & Manojkumar, T. K. (2021), ExplAoring the selectivity of guanine scaffold in anticancer drug development by computational repurposing approach. Sci. Rep, 11, 16251.

[4] Kadkol, H., Jain, V. & Patil, A. B. (2019). Multi-drug resistance in cancer therapy-An overview. J. Crit. Rev, 6 (6),1e6. S.

[5] Dallavalle, V., Dobricic, L., Lazzarato, E., Gazzano, M., Machuqueiroe, I., Pajeva, I., Tsakovska, N & Zidar, R. F. (2020). Improvement of conventional anti-cancer drugs as new tools against multidrug resistant tumors, Drug Resist. Updates, 50, e100682.

[6] Falzone, L., Salomone, S., Libra, M. (2018). Evolution of cancer pharmacological treatments at the turn of the third millennium. Front. Pharmacol. 9, 1300.

[7] Kamaraju, S., Drope, J., Sankaranarayanan, R., & Shastri, S. (2020). Cancer prevention in low-resource countries: an overview of the opportunity. *American Society of Clinical Oncology Educational Book*, *40*, 72-83.

[8] Soheili, M., Keyvani, H., Soheili, M. & Nasseri, S. (2021). Human papilloma virus: A review study of epidemiology, carcinogenesis, diagnostic methods, and treatment of all HPV-related cancers. Med J Islam Repub Iran, 22, 35-65. doi: 10.47176/mjiri.35.65.

[9] Farmer, E., Cheng, M. A., Hung, C. F. & Wu, T. C. (2021). Vaccination Strategies for the Control and Treatment of HPV Infection and HPV-Associated Cancer. Recent Results Cancer Res, 217, 157-195. doi: 10.1007/978-3-030-57362-1_8.

[10] Han, L. & Zhang, B. (2023). Can prophylactic HPV vaccination reduce the recurrence of cervical lesions after surgery? Review and prospect. *Infect Agents Cancer,* 18, 66. https://doi.org/10.1186/s13027-023-00547-2

[11] Jabbour, E. & Kantarjian, H. (2022). Chronic myeloid leukemia: 2022 update on diagnosis, therapy, and monitoring. Am J Hematol, 97(9), 1236-1256. doi: 10.1002/ajh.26642. Epub 2022 Jul 6.

[12] Shyam Sunder, S., Sharma, U. C., & Pokharel, S. (2023). Adverse effects of tyrosine kinase inhibitors in cancer therapy: pathophysiology, mechanisms and clinical management. *Signal*

Transduction and Targeted Therapy, *8*(1), 262.

[13] Jacobs, C. F., Eldering, E. and Kater, A. P. (2021). Kinase inhibitors developed for treatment of hematologic malignancies: implications for immune modulation in COVID-19. Blood Adv. 5(3), 913-925. doi: 10.1182/bloodadvances.2020003768.

[14] Waarts, M. R., Stonestrom, A. J, Park, Y. C., Levine, R. L. (2022). Targeting mutations in cancer. J Clin Invest. 132(8), e154943. doi: 10.1172/JCI154943.

[15] Pandrala, M., Bruyneel, A. A. N., Hnatiuk, A. P., Mercola, M., & Malhotra, S. V. (2022). Designing novel BCR-ABL inhibitors for chronic myeloid leukemia with improved cardiac safety. *Journal of medicinal chemistry*, *65*(16), 10898-10919.

[16] Dhyani, P., Quispe, C., Sharma, E., Bahukhandi, A., Sati, P., Attri, D. C., ... & Cho, W. C. (2022). Anticancer potential of alkaloids: a key emphasis to colchicine, vinblastine, vincristine, vindesine, vinorelbine and vincamine. *Cancer cell international*, *22*(1), 206.

[17] Zandavar, H., & Afshari Babazad, M. (2023). Secondary Metabolites: Alkaloids and Flavonoids in Medicinal Plants. IntechOpen. doi: 10.5772/intechopen.108030

[18] Kumar, A., Singh, A.K., Singh, H., Vijayan, V., Kumar, D., Naik, J., Thareja, S., Yadav, J.P., Pathak, P. and Grishina, M. (2023). Nitrogen Containing Heterocycles as Anticancer Agents: A Medicinal Chemistry Perspective. *Pharmaceuticals*, *16*, 299. https://doi.org/10.3390/ph16020299

[19] Ceramella, J., Iacopetta, D., Barbarossa, A., Caruso, A., Grande, F., Bonomo, M. G., ... & Sinicropi, M. S. (2020). Carbazole derivatives as kinase-targeting inhibitors for cancer treatment. *Mini Reviews in Medicinal Chemistry*, *20*(6), 444-465.

[20] Beniwal, S. C., & Virmani (2023), T. Recent Advancement of Carbazole Hybrid: A Privileged Scaffold in New Drug Discovery seem a Chahar Beniwal and Tarun Virmani Beniwal and Virmani, International Journal of Pharmaceutical Sciences and Research, 14(3), 1054-1062.

[21] Grande, F., Ioele, G., Caruso, A., Occhiuzzi, M. A., El-Kashef, H., Saturnino, C. & Sinicropi, M. S. (2023). Carbazoles: Role and Functions in Fighting Diabetes. *Appl. Sci, 13*, 349. https://doi.org/10.3390/app13010349

[22] Ozer, E. B., Caglayan, C., & Bayindir, S. (2022). The solvent-controlled regioselective synthesis of 3-amino-5-aryl-rhodanines as novel inhibitors of human carbonic anhydrase enzymes. *Tetrahedron*, *120*, 132896. https://doi.org/10.1016/j.tet.2022.132896.

[23] Sharma, A., Sharma, D., Saini, N., Sharma, S. V., Thakur, V. K., Goyal, R. K., & Sharma, P. C. (2023). Recent advances in synthetic strategies and SAR of thiazolidin-4-one containing molecules in cancer therapeutics. *Cancer and Metastasis Reviews*, *42*(3), 847-889.

[24] Mermer A. (2021). The Importance of Rhodanine Scaffold in Medicinal Chemistry: A Comprehensive Overview. Mini Rev Med Chem, 21(6), 738-789. doi: 10.2174/1389557521666201217144954.

[25] Liu, H., Sun, D., Du, H., Zheng, C., Li, J., Piao, H., ... & Sun, L. (2019). Synthesis and biological evaluation of tryptophan-derived rhodanine derivatives as PTP1B inhibitors and anti-bacterial agents. *European Journal of Medicinal Chemistry*, *172*, 163-173.

[26] Boureghda, C., Boulcina, R., Dorcet, V., Berrée, F., Carboni, B., & Debache, A. (2021). Facile synthesis of 5-arylidene rhodanine derivatives using Na2SO3 as an eco-friendly catalyst. Access to 2-mercapto-3-aryl-acrylic acids and a benzoxaborole derivative. *Tetrahedron letters*, *62*, 152690.

[27] Yararli, K., Ozer, E. B., Bayindir, S., Caglayan, C., Turkes, C., & Beydemir, S. (2023). The synthesis, biological evaluation and in silico studies of asymmetric 3, 5-diaryl-rhodanines as novel inhibitors of human carbonic anhydrase isoenzymes. *Journal of Molecular Structure*, *1276*, 134783.

https://doi.org/10.1016/j.molstruc.2022.134783.

[28] Krátký, M., Štěpánková, Š., Vorčáková, K., & Vinšová, J. (2016). Synthesis and in vitro evaluation of novel rhodanine derivatives as potential cholinesterase inhibitors. *Bioorganic Chemistry*, *68*, 23-29.

[29] Yang, N., Ren, Z., Zheng, J., Feng, L., Li, D., Gao, K., ... & Zuo, P. (2016). 5-(4-hydroxy-3-dimethoxybenzylidene)-rhodanine (RD-1)-improved mitochondrial function prevents anxiety-and depressive-like states induced by chronic corticosterone injections in mice. *Neuropharmacology*, *105*, 587-593.

[30] Chauhan, D., George, G., Sridhar, S. N. C., Bhatia, R., Paul, A. T., & Monga, V. (2019). Design, synthesis, biological evaluation, and molecular modeling studies of rhodanine derivatives as pancreatic lipase inhibitors. *Archiv der Pharmazie*, *352*(10), 1900029.

[31] S.K. Celestina, K. Sundaram, S. Ravi, In vitro studies of potent aldose reductase inhibitors: synthesis, characterization, biological evaluation and docking analysis of rhodanine-3-hippuric acid derivatives, Bioorg. Chem, 97 (2020), 103640.

[32] Singhm, A. K, Kumar, A., Singh, H., Sonawane, P., Paliwal, H., Thareja, S., Pathak, P., Grishina, M., Jaremko, M., Emwas, A.H., Yadav. J.P., Verma, A., Khalilullah, H. & Kumar, P. (2022). Concept of Hybrid Drugs and Recent Advancements in Anticancer Hybrids. Pharmaceuticals (Basel), 28 (9), 1071. doi: 10.3390/ph15091071.

[33] Alkhzem, A. H., Woodman, T. J., & Blagbrough, I. S. (2022). Design and synthesis of hybrid compounds as novel drugs and medicines. *RSC advances*, *12*(30), 19470-19484.

[34] Pinheiro, P. S. M., Franco, L. S. Tadeu, Montagnoli, L., Alberto, C. & Fraga, M. (2024). Molecular hybridization: a powerful tool for multitarget drug discovery, Expert Opinion on Drug Discovery, 19 (4), 451-470.

[35] Erazua, E. A., Oyebamiji, A. K. and Adeleke, B. B. (2018). DFT-QSAR and Molecular Docking Studies on 1,2,3-Triazole-Dithiocarbamate Hybrids as Potential Anticancer Agents. Physical Science International Journal, 20 (4): 1-10.

[36] Erazua, E. A., Akintelu, S. A., Adelowo, J. M., Odoemene, S. N., Josiah, O. M., Raheem, S. M., Latona, D. F., Adeoye, M. D., Esan, A. O. & Oyebamiji, A. K. (2021). QSAR and Molecular Docking Studies on Nitro (Triazole/Imidazole)-Based Compounds as AntiTubercular Agents, Tropical Journal of Natural Product Research, 5(11), 2022-2029.

[37] Jiang, H., Zhang, W. J., Li P. H., Wang, J., Dong, C. Z., Zhang, K., Chen, H. X., Du, & Z. Y. (2018). Synthesis and biological evaluation of novel carbazole-rhodanine conjugates as topoisomerase II inhibitors. Bioorg Med Chem Lett, 28(8),1320-1323. doi: 10.1016/j.bmcl.2018.03.017.

[38] Kim, D., Chin, M., Yu, H., Pan, X., Bian, H., Tan, Q., Kahn, R, A., Tsigaridis, K., Bauer, S. E., Takemura, T., Pozzoli, L., Bellouin, N. & Schulz, M. (2019). Asian and trans-Pacific Dust: a multi-model and multiremote sensing observation analysis. J Geophys Res Atmos, 124 (23), 13534-13559. https:// doi. org/ 10. 1029/ 2019J D0308 22

[39] O'Boyle, N. M., Banck, M., James, C. A., Morley, C., Vandermeersch, T. & Hutchison, G. R. (2011). Open Babel: An open chemical toolbox. J Cheminform, 7(3), 33. doi: 10.1186/1758-2946-3-33. PMID: 21982300; PMCID: PMC3198950.

[40] Genera, M., Samson, D., Raynal, B., Haouz, A., Baron, B., Simenel, C., Guerois, R., Wolff, N. & Caillet-Saguy, C. (2019). Structural and functional characterization of the PDZ domain of the human phosphatase PTPN3 and its interaction with the human papillomavirus E6 oncoprotein. Sci Rep, 9, 7438-7438.

[41] Liu, F., Wang, B., Wang, Q., Qi, Z., Chen, C., Kong, L. L., Chen, J. Y., Liu, X., Wang, A., Hu, C., Wang, W., Wang, H., Wu, F., Ruan, Y., Qi, S., Liu, J., Zou, F., Hu, Z., Wang, W., Wang, L., Zhang, S., Yun, C.H., Zhai, Z., Liu, J. & Liu, Q. Discovery

and characterization of a novel potent type II native and mutant BCR-ABL inhibitor (CHMFL-074) for Chronic Myeloid Leukemia (CML). Oncotarget, 7: 45562-45574

[42] Pettersen, E. F., Goddard, T. D., Huang, C. C., Couch, G. S., Greenblatt, D. M., Meng, E. C. & Ferrin, T. E. (2004). UCSF Chimera—a visualization system for exploratory research and analysis. Journal of computational chemistry, 25(13), 1605-1612.

[43] Trott, O. & Olson, A. J. (2010). AutoDock Vina: Improving the speed and accuracy of docking with a new scoring function, efficient optimization, and multithreading. J Comput Chem, 31(2), 455-461.

[44] Valdés-Tresanco, M. S., Valdés-Tresanco, M. E., Valiente, P. A., Moreno, E, (2020). AMDock: a versatile graphical tool for assisting molecular docking with Autodock Vina and Autodock4. Biology direct, 2020, 15(1), 1-12.

[45] Erazua, E. A., Adepoju, A. J., Ajayi, A. P, Josiah O. M., Akintelu, S. A. and Oyebamiji, A. K. (2021). Theoretical Studies on Triazoles of 3-Acetylbetulin and Betulone as Anticancer Agents. Nature and Science, 19(7):5-18.

[46] Guan, L., Yang, H., Cai, Y., Sun, L., Di, P., Li, W., Liu, G., Tang, Y. (2018). ADMET-score - a comprehensive scoring function for evaluation of chemical drug-likeness. Med Chem. Comm, 30 (1), 148-157. doi: 10.1039/c8md00472b. PMID: 30774861.

[47] Erazua, E. A., Oyebamiji, A. K., Akintelu, S. A., Adewole, P. D., Adelakun, A. & Babatunde Benjamin Adeleke. (2023). Quantitative Structure-Activity relationship, Molecular Docking and ADMET Screening of Tetrahydroquinoline Derivatives as AntiSmall Cell Lung Cancer Agents. Eclética Química, 48(1), 55-71.

[48] Lipinski, C. A. M, Lombardo, F., Dominy, B. W. & Feeney, P. J, (2001), Experimental and computational approaches to estimate solubility and permeability in drug discovery and development settings. Adv. Drug Deliv. Rev, 46(1-3), 3-26. https://doi.org/10.1016/S0169-409X(00)00129-0

[49] Veber, D. F., Johnson, S. R., Cheng, H. Y., Smith, B. R., Ward, K. W. & Kopple, K. D. Molecular properties that influence the oral bioavailability of drug candidates. J. Med. Chem. 2002, 45 (12), 2615-2623 https://doi.org/10.1021/jm020017n.

[50] Egan, W. J., Merz, K. M. & Baldwin, J J. (2000). Prediction of Drug Absorption Using Multivariate Statistics. *J. Med. Chem, 43*, 3867-3877.

[51] Muegge, I. (2002). Pharmacophore features of potential drugs. *Chemistry–A European Journal*, *8*(9), 1976-1981.

[52] Sazonova, E. V., Chesnokov, M. S., Zhivotovsky, B. & Kopeina, G. S. (2022). Drug toxicity assessment: cell proliferation versus cell death. Cell Death Discov, 14(1), 417. doi: 10.1038/s41420-022-01207-x.

[53] Daina, A., Michielin, O. & Zoete, V. (2017). SwissADME: A free web tool to evaluate pharmacokinetics, drug-likeness and medicinal chemistry friendliness of small molecules. Sci. Rep, 75 (1), 56-63. https://doi.org/10.1038/srep42717 es 07,

[54] Banerjee, P, Eckert, A. O., Schrey, A. K. & Preissner, R. (2018). ProTox-II: a webserver for the prediction of toxicity of chemicals. Nucleic Acids Res. 46(1), 257-263. https://doi.org/10.1093/nar/gky318.

[55] Skoraczyński, G., Kitlas, M., Miasojedow, B., & Gambin, A. (2023). Critical assessment of synthetic accessibility scores in computer-assisted synthesis planning. *Journal of Cheminformatics*, *15*(1), 6.

[56] Jeevana, R., Kavitha, A. P., Abi, T. G., Sajith, P. K., Varughese, J. K. & Aravindakshan, K. K. (2022). Targeting COVID-19 pandemic: in silico evaluation of 2-hydroxy-1, 2-diphenylethanone N(4)-methyl-N(4)-phenylthiosemicarbazone as a potential inhibitor of SARS-CoV-2. Struct Chem, 17, 1-17. doi: 10.1007/s11224-022-02033-8.

[57] Morak-Młodawska, B., Jeleń, M., Martula, E. & Korlacki, R. (2023). Study of Lipophilicity and ADME Properties of 1,9-Diazaphenothiazines Anticancer Action.

Int J Mol Sci. 9 (8), 6970. doi: 10.3390/ijms24086970.

[58] Johnson, T. O., Adegboyega, A. E., Iwaloye, O., Eseola, O. A., Plass, W., Afolabi, B., Rotimi, D., Ahmed, E., Albrakati, A., Batiha, G. E. & Adeyemi, O. S. (2021). Computational study of the therapeutic potentials of a new series of imidazole derivatives against SARS-CoV-2. J. Pharmacol. Sci, 147 (1), 62-71. https://doi.org/10.1016/j.jphs.2021.05.004

[59] Ahmad, I., Kuznetsov, A. E., Pirzada, A. S., Alsharif, K. F., Daglia, M. & Khan, H. 2023. Computational pharmacology and computational chemistry of 4-hydroxyisoleucine: Physicochemical, pharmacokinetic, and DFT-based approaches. Front Chem. 13(11), 1145974. doi: 10.3389/fchem.2023.1145974.

[60] Wu, f., Zhou, Y., Li, L., Shen, X., Chen, G., Wang, X., Liang, M., Tan, M. & Huang, M. (2020). Computational Approaches in Preclinical Studies on Drug Discovery and Development, Front Chem. 11: 726, doi: 10.3389/fchem.2020.00726.

[61] Mokgautsi, N., Wen, Y., Lawal, B., Khedkar, H., Sumitra, M. R, Wu, W. & Huang, H. S. (2021). An Integrated Bioinformatics Study of a Novel Niclosamide Derivative, NSC765689, a Potential *GSK3β/β-Catenin/STAT3/CD44* Suppressor with Anti-Glioblastoma Properties. *Int. J. Mol. Sci.* 22, 2464, https://doi.org/10.3390/ijms22052464.

[62] Dahan, A., & González-Álvarez, I. (2021). Regional intestinal drug absorption: Biopharmaceutics and drug formulation. *Pharmaceutics*, *13*(2), 272.

[63] Kadry, H., Noorani, B., & Cucullo, L. (2020). A blood–brain barrier overview on structure, function, impairment, and biomarkers of integrity. *Fluids and Barriers of the CNS*, *17*, 1-24.

[64] Shchulkin, A., Abalenikhina, Y.V., Erokhina, P. D., Chernykh, I.V. & Yakusheva. E. N. (2021). The Role of P-Glycoprotein in Decreasing Cell Membranes Permeability during Oxidative Stress. Biochemistry (Mosc), 86 (2), 197-206, doi: 10.1134/S0006297921020085.

[65] Zhao, M., Ma, J., Li, M., Zhang, Y., Jiang, B., Zhao, X., ... & Qin, S. (2021). Cytochrome P450 enzymes and drug metabolism in humans. *International journal of molecular sciences*, *22*(23), 12808.

[66] Erazua, E. A., and Adelekea, B.B. (2024). Antioxidan t, Anti-Inflammatory and Anti-Glycation Activities of Some 4-Aminoantypyrine Derivatives: In Vitro and in Silico Study. JOPAT. 23(1) 1313-1347, https://dx.doi.org/10.4314/jopat.v23i1.9.

[67] Souto, E. B., Fangueiro, J. F., Fernandes, A. R., Cano, A., Sanchez-Lopez, E., Garcia, M. L., ... & Silva, A. M. (2022). Physicochemical and biopharmaceutical aspects influencing skin permeation and role of SLN and NLC for skin drug delivery. *Heliyon*.

[68] Iyer, A., Jyothi, V. G. S., Agrawal, A., Khatri, D. K., Srivastava, S., Singh, S. B., & Madan, J. (2021). Does skin permeation kinetics influence efficacy of topical dermal drug delivery system?: Assessment, prediction, utilization, and integration of chitosan biomacromolecule for augmenting topical dermal drug delivery in skin. *Journal of Advanced Pharmaceutical Technology & Research*, *12*(4), 345-355.

[69] Hammami, M., Chaabani, E., Yeddes, W., Wannes, W. A., & Bourgou, S. (2023). Phenolic Compounds and Skin Permeability: An In Silico Investigation. *Avicenna Journal of Medical Biochemistry*, *11*(1), 11-18.

[70] Sun, J., Yu, X., Weng, Z., Jin, L., Yang, J., Zhang, H., ... & Yang, J. (2022). The impact of hepatotoxic drugs on the outcome of patients with acute deterioration of hepatitis B virus-related chronic disease. *European Journal of Gastroenterology & Hepatology*, *34*(7), 782-790.

[71] Liu, S., Saunders, M., & Mak, T. W. (2023). Chemical carcinogens: implications for cancer treatment. *Journal of Clinical Investigation*, *133*(20), e174319.

[72] Bou Zerdan, M., Moussa, S., Atoui, A., & Assi, H. I. (2021). Mechanisms of

immunotoxicity: stressors and evaluators. *International Journal of Molecular Sciences*, *22*(15), 8242